Proceedings of 2018 IEEE
International Conference on Mechatronics and Automation
August 5 - 8, Changchun, China

Catheter Tracking Based on Multi-scale Filter and Direction-oriented Method

Yuwen Zeng[1], Nan Xiao[1]*, Shuxiang Guo[1,2], Yan Zhao[1], Yuxin Wang[1]
[1] *Key Laboratory of Convergence Biomedical Engineering System and Healthcare Technology, The Ministry of Industry and Information Technology, School of Life Science, Beijing Institute of Technology, No.5, Zhongguancun South Street, Haidian District, Beijing 100081, China*
[2] *Faculty of Engineering, Kagawa University, 2217-20 Hayashi-cho, Takamatsu, Kagawa 760-8521, Japan*
E-Mails:{2120171402 & xiaonan }@bit.edu.cn;
* Corresponding author

***Abstract* - Nowadays the morbidity and mortality of cardiovascular and cerebrovascular diseases are increasing year by year. Vascular interventional surgery has been considered as the most widely treatment to these diseases and it is developing rapidly for its minimally invasive procedure, safety and short recovery time. However, due to the low signal-to-noise ratio (SNR) and pipe-like structures in the human body, the resolution of fluoroscopic sequences can be too low for surgeons to recognize the catheter in some cases, which impose restrictions on the performance and efficiency of this surgery in clinic. Therefore, enhancing and tracking the catheter in the endovascular interventions have become a crucial part. This paper proposes a morphologic method based on multiscale filter and direction-oriented method, which can enhance and detect the catheter from sequences in real-time. And finally this method takes 0.064s per frame with an accuracy of 89.39%, which can meet the requirements of clinic operations.**

Index Terms – Vascular interventional surgery, Multi-scale enhancement, Direction-oriented, Morphology

I. INTRODUCTION

Cardiovascular and cerebrovascular disease is one of the most common diseases of mankind that threaten human's life and vascular interventional surgery has become a major method to treat these diseases[1],[2]. In the traditional interventional procedures, catheter tracking can provide the doctor with visual information [3]. The current interventional robotic system is based on the DSA (Digital Subtraction Angiography) information and the surgeons master the slave robot to perform the operation [4]. However, the research of the existing vascular interventional robot system mainly focuses on the master-slave operation function [5], force feedback[6],[7] and virtual surgical system[8], so the research on catheter tracking is also meaningful. In the interventional surgery, surgeons observe the position of catheter under the X-ray, and make a contrast if necessary to obtain the structure of blood vessels [9], [10]. So one of the key requirements for such surgeon is the accurate positioning of the catheter. However, the guidewire is a non-rigid 1-D structure, which means it is prone to deform in anyway.The low dose used in fluoroscopy that aims to reduce the harm to patients and surgeons for being exposed to the X-ray introduce limitations to image quality. Meanwhile, the breath motion of patients leads to image artifacts which increase the difficulty on target detection, and pipe-like structures such as skeleton and the edge of organs also introduce noises into the images [11].

Fig. 1. The demonstration of vascular interventional surgery

There are mainly two navigation systems for vascular interventional surgery: electromagnetic system and traditional system [12]. However, magnetic navigation technology is still in the development stage, and it cannot completely replace the current traditional intervention surgery. The diameter of the magnetic navigation catheter is not thin enough to enter the small in surgeries. Since the magnetic navigation system is expensive, the cost of an electrophysiology catheterization room equipped with a magnetic navigation system is about 3 times that of a conventional room, which is one of the reasons that the magnetic navigation system has encountered obstacles in popularization [13].

In the traditional system, the most popular method for guidewire and catheter tracking is the B-spline fitting. Ping-Lin Chang et al. proposed a deformable B-spline tube model probabilistic optimisation framework which can effectively represent the shape of a catheter and it took about 50 ms for 10 knot points [14]. Shirley A. M. Baert developed a method using a template-matching procedure and determining the position of the guidewire by fitting a spline to a feature image with manual outlining. And it took 5s per frame with an average accuracy of around 90% [15]. Hauke Heibel et al. presented an approach based on modeling catheter with B-splines whose optimal configuration of control points was determined through efficient discrete optimization. Each control point corresponded to a discrete random variable in a Markov random field formulation [16]. Cheng Wang et al. proposed a method of open active contour based on edge detection and an algorithm for deforming and control of

curves. And the results showed that the accuracy rate was 95.3% from the clinical images. However their study was focus on a single frame and got a speed of 3.8s per frame [17]. H.R. Fazlali et al. smoothed each frame using guided filter. The catheter was detected in the first frame using Hough transform, then they fit a second order polynomial on the catheter and accurately tracked it throughout the sequence [18]. Slabaugh G et al. presented equations that deformed a spline, subjected to intrinsic and extrinsic forces, so that it matched the image data and remained smooth by using the variational calculus and phase congruency as an image-based feature [19]. Jiong Zhang et al. used an orientation scores in retinal vessel segmentation that was capable of dealing with typically difficult cases like crossings, central arterial reflex, closely parallel and tiny vessels [20]. Mohammed Shafeeq Ahmed describe a procedure for automatic detection of MAs by applying threshold and mathematical morphology techniques [21]. J Yang proposed an improved Hessian multiscale filter. An image grayscale factor is added to the vascular similarity function computed by Hessian matrix eigenvalue [22]. Jian Zheng et al. employed a multiscale Hessian-based filter to compute the maximum response of vessel likeness function for each pixel. After that, a radial gradient symmetry transformation is adopted to suppress the non-vessel structures [23]. Xu X first decomposed the angiogram into several directional images and each of them is enhanced by traditional Hessian-based method. Then the enhanced direction images are recombined to generate final result [24].

Also, there are some studies using machine learning methods. L wang et al. a novel image-based fully-automatic approach with convolutional neural network for guide-wires detection. The detection accuracy evaluated by average precision (AP) reaches 89.2%. However, it takes a lot of time to label every frame and the dataset is not available to public [25]. Barbu A et al. learned the complex shape and appearance of a free-form curve using a hierarchical model of curves and a database of manual annotations, and then used a computational paradigm in the context of Marginal Space Learning, in which the algorithm was closely integrated with the hierarchical representation. This method had a processing speed of 1frame per second, and they got an accuracy of 68% on 535 images and an error of less than 1mm [26].

In conclusion, for machine learning methods, especially the deep learning method, those well-trained model will obviously cut the time for detecting and tracking. However, it would take a long period for collecting origin image, labelling large amount of data and training models. And if the dataset is not large enough, we may get an overfitting model which has a poor generalization ability. On the other hand, the approaches such as B-spline fitting, open active contour and other modelling ways show good results and high accuracy on catheter detecting and tracking. But the performance of an algorithm often goes against with the processing time. In order to fit the curve accurately in each frame, the computer needs to do a lot of calculations, therefore these kinds of method can hardly meet the clinic requirement of real-time.

In this paper, we present a catheter tracking method based on multiscale filter and direction-oriented algorithm, which can enhance and detect the catheter in real-time. In section II, the enhancing and detecting method is elaborated. In section Ⅲ, the performance evaluation experiments are conducted and the result is discussed. In section Ⅳ, the research work is concluded and the future work is pointed out.

II. Design of the Real-Time Detecting System

To reduce the noise in the fluoroscopic images, we apply a nonlinear digital filtering technique to remove noise and smooth every single frame so that to improve the results of later processing. Then we use a multi-scale filter and a black-Tophat (only when the background is complex) transform to enhance the catheter in the image, and further screen out the redundant information of the pattern through a direction-oriented filter. Finally, the morphological method is used as post-processing.

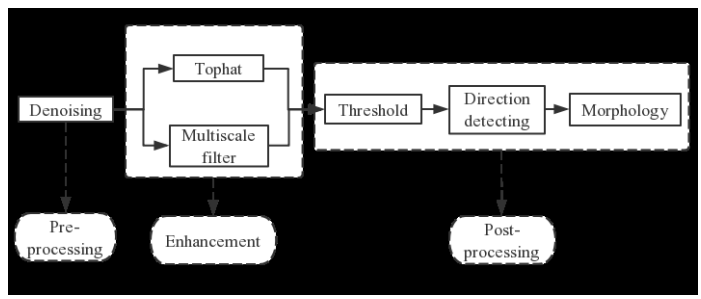

Fig. 2. Algorithm flowchart

A. Multi-scale Filter based on Hessian matrices

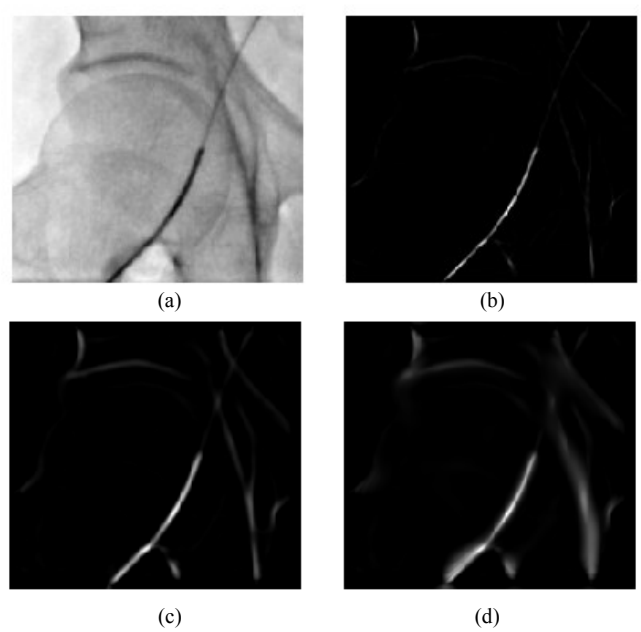

Fig. 3. Catheter enhanced by Hessian matrix with different scales. (a) is the origin image of a fluoroscopy; (b) is with scale = (1,2); (c) is with scale = (1,5); (d) is with scale = (1,10).

Image enhancement methods based on Hessian matrices are most commonly used to enhance tubular or linear structures such as blood vessels, rivers and wrinkles, including the Frangi algorithm [27-29], the Lorenz algorithm, etc. The idea of multi-scale representation is to integrate the original signal into a series of signals that can be obtained through single-parameter transformation [30]. Each signal corresponds to one parameter in a single-parameter class. The scale can be obtained by smoothing and only the second-order Gaussian function is available, where σ is the standard deviation of the function. The value of σ determines the smoothness of the image, the large σ value represents the image contour feature, and the small σ value represents the image detail feature.

As is shown in Fig. 3, we have enhanced the image with different scales. Each single scale has a good enhancement effect only on the place that best matches the current scale, but when the catheter scale does not match the current scale or does not exactly match, the filter has almost no enhancement effect on the it. Therefore, using multi-scale filter can achieve effective enhancement of catheters at various scales in the image. A proper scale step can be set up to adjust how the σ increases, and if a small step is chosen, we may get a better match at the cost of time.

To determine whether a point X belongs to the target, we need to analyze the Taylor expansion of this point $P=(x,y)$ in the neighborhood of the image $I(x,y)$:

$$I(P+\Delta P)\approx I(P)+\Delta P^T\nabla I(\mathrm{P})+\Delta P^T H(P)\Delta P \tag{1}$$

where ΔP is the variation of point P in one of its neighborhood, $\nabla I(\mathrm{P})$ is the gradient of the image at point P. $H(P)$ is the Hessian matrix of P, which consists of the second-order partial derivative of this point:

$$H(P)=\begin{bmatrix} I_{xx}(P) & I_{xy}(P) \\ I_{yx}(P) & I_{yy}(P) \end{bmatrix} \tag{2}$$

And it has two eigenvalues λ_1 and λ_2. If $|\lambda_1|>>|\lambda_2|\approx 0$, it means that there are pipe-like structures around this pixel. And this is how the filter builds [31]:

$$v_0(x,y)=\max_{\sigma_{\min}\le\sigma\le\sigma_{\max}} v(x,y;\sigma) \tag{3}$$

$$v(x,y;\sigma)=\begin{cases} 0, if\ \lambda_1>0 \\ e^{-\frac{R_\alpha^2}{2\alpha^2}}(1-e^{-\frac{R_\beta^2}{2\beta^2}}), if\ \lambda_1\le 0 \end{cases} \tag{4}$$

$$R_\alpha=\left(\frac{\lambda_1}{\lambda_2}\right)^2, R_\beta=\sqrt{\lambda_1^2+\lambda_2^2} \tag{5}$$

where R_α distinguishes between blob-like and pipe-like structures, R_β distinguishes the foreground and background. α and β are the Frangi correction constants that adjusts the filter's sensitivity to deviation from a blob-like structure to areas of high variance, respectively. And α is the crucial parameter that determines how the catheter is detected.

The Frangi algorithm is based on Sato and Lorenz's. Compared with Lorenz, it takes all the eigenvalues into account and interprets the pipe-like features geometrically [32]. In Fig. 4, The structure of the catheter firstly becomes clearer and then blurred as the α increases gradually. During such a process of rising and decreasing, the highest value of the response is the one that best matches the target structure. In this paper, we choose the 0.5 as the value of α.

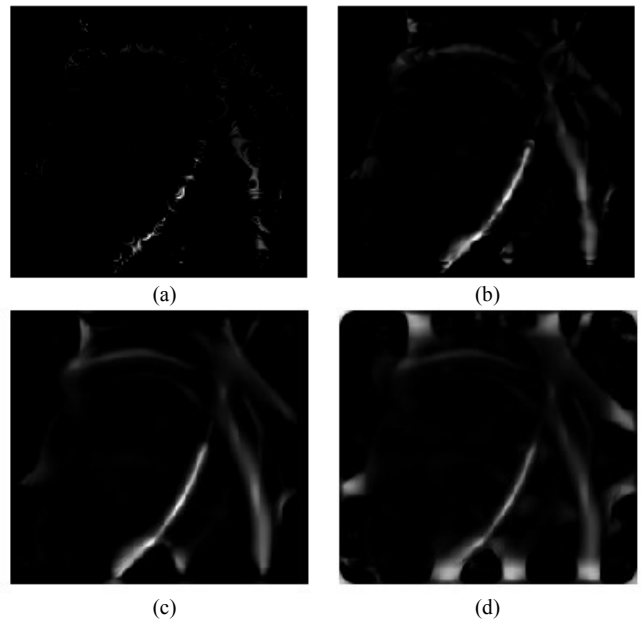

Fig. 4. Catheter enhanced by Hessian matrix. (a) is with α = 0.01; (b) is with α = 0.1; (c) is with α = 0.5; (d) is with α = 5.

B. Direction-oriented Method

The gradation of the place where there is an edge in the image is a gentle-steep-gentle curve, which means the slope of the gradation curve at the edge is larger. A good way to express changes is by using derivatives. Similarly, if we only detect gray changes in one direction, for example, the longitudinal features, then we just need to calculate the x-order partial derivative the image, so that those horizontal edge will not be detected. For edge detecting operator, Sobel shows good performance [33-35].

$$\text{Sobel: } G_x=\begin{bmatrix} -1 & 0 & -1 \\ -2 & 0 & -2 \\ -1 & 0 & -1 \end{bmatrix} \tag{6}$$

However, when the size of the kernel is 3, the Sobel kernel shown above may produce noticeable inaccuracies since it is only an approximation of the derivative. OpenCV addresses this inaccuracy for kernels of size 3 by using the Scharr function. This is as fast but more accurate than the Sobel operator.

$$\text{Scharr: } G_x=\begin{bmatrix} -3 & 0 & -3 \\ -10 & 0 & -10 \\ -3 & 0 & -3 \end{bmatrix} \tag{7}$$

During interventional surgeries, clips and other items on

the patients' clothing are shown under x-rays. The clips are also linear objects and therefore detected by the filter (Fig. 5 (a)). To remove these kinds of unrelated feature, the image is directional filtered to remove them in different directions. As Fig. 5(b) shows, there exists the feature from a clip that we can't remove it easily by applying a threshold. So the horizontal changes (Fig. 5(c)) are computed by convolving the image with the kernel G_x.

(a) (b) (c)

Fig. 5. Disturbance from pipe-like structure. (a) is the origin image; (b) is the image enhanced; (c) is the image after directional filtering.

C. Morphology-based Post-processing

Mathematical morphology uses a structural element with a certain shape, size, and other characteristics to detect an image. The structural element is similar to a probe that directly carries information such as direction, size and chromaticity. It can be used to detect the positions of image where match or response to the structural elements, extract valuable information from images for the purpose of analyzing and identifying images.

In most cases, the target object has the largest area ratio in the image, so at the end we remove all non-catheter information by detecting the area of all connected fields in the graph and deleting all the blobs smaller than the maximum area. After the directional filtering applied to remove lateral textures, there remain many residual fragments in the image, and local discontinuities may occur on the catheters, which will affect the correct calculation of the maximum area. So first we make a closing on the image. In mathematical morphology, the closing of a set A by a structuring element B is the erosion of the dilation of that set:

$$A \bullet B = (A \oplus B) \Theta B \tag{8}$$

where $\oplus$ and Θ denote the dilation and erosion, respectively. They are two basic algorithms in morphology. Dilation refers to adding some pixels to the edge of the ROI (region of interest) in the image:

$$(A \oplus B)(x,y) = \max\left\{ A(x-x', y-y') + B(x',y') \,\middle|\, \begin{matrix} (x-x')(y-y') \in D_A \\ (x',y') \in D_B \end{matrix} \right\} \tag{9}$$

while erosion removes certain edge information:

$$(A \Theta B)(x,y) = \max\left\{ A(x+x', y+y') - B(x',y') \,\middle|\, \begin{matrix} (x+x')(y+y') \in D_A \\ (x',y') \in D_B \end{matrix} \right\} \tag{10}$$

In Fig. 6, after connecting the discontinuous part that may occur on the catheter, a thin operation is applied to the image so as to reduce the calculation. The final step of morphology is to label all the connected domain and calculate the maximum area which is chosen as the threshold to remove other smaller domain.

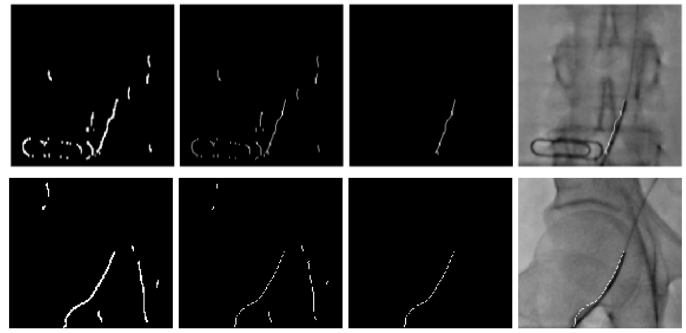

(a) (b) (c) (d)

Fig. 6. The post-processing and final result. s(a) is the image after directional filtering; (b) is the image applied with thin operation; (c) is the image after removing other smaller area; (d) is the final result.

III. Experiment and Results

To assess the performance of proposed catheter detecting and tracking system, 2 sequences totaling 283 images are used. These sequences are obtained from two endovascular surgeries in Beijing Tiantan Hospital and the procedure is from the femoral artery to the carotid artery. Since this paper focuses on the real-time system, rather than the authoritative evaluation method presented in [14], we present the quantitative results by computing the true positive and false positive as is in [17]:

Using these measurements we summarize the evaluation results in Table. 1 .

TABLE. 1 Evaluation Results

No.	TP	FP
Seq.1	142	19
Seq.2	111	11
Over-all	89.39%	10.61%

The algorithm takes about 0.064s per frame, which means it can achieve more than 15fps (frame per second) that researches the requirement of clinical application for endovascular interventional surgery, much faster than 1fps and 0.26fps mentioned before. Finally, we achieve an over-all accuracy of 89.39%. Table. 2 shows the comparison of results among several related work mentioned in part I.

TABLE. 2 Comparison of results

Paper No.	Tracking success	Processing speed	Tracking Method
[14]	90%	0.2fps	B-spline
[16]	95.3%	0.26fps	B-spline
[17]	95.9%	Not mentioned	Polynomial fitting
[25]	68%	1fps	Machine Learning
Proposed method	89.39	15.6fps	Multi-scale filter and directional filter

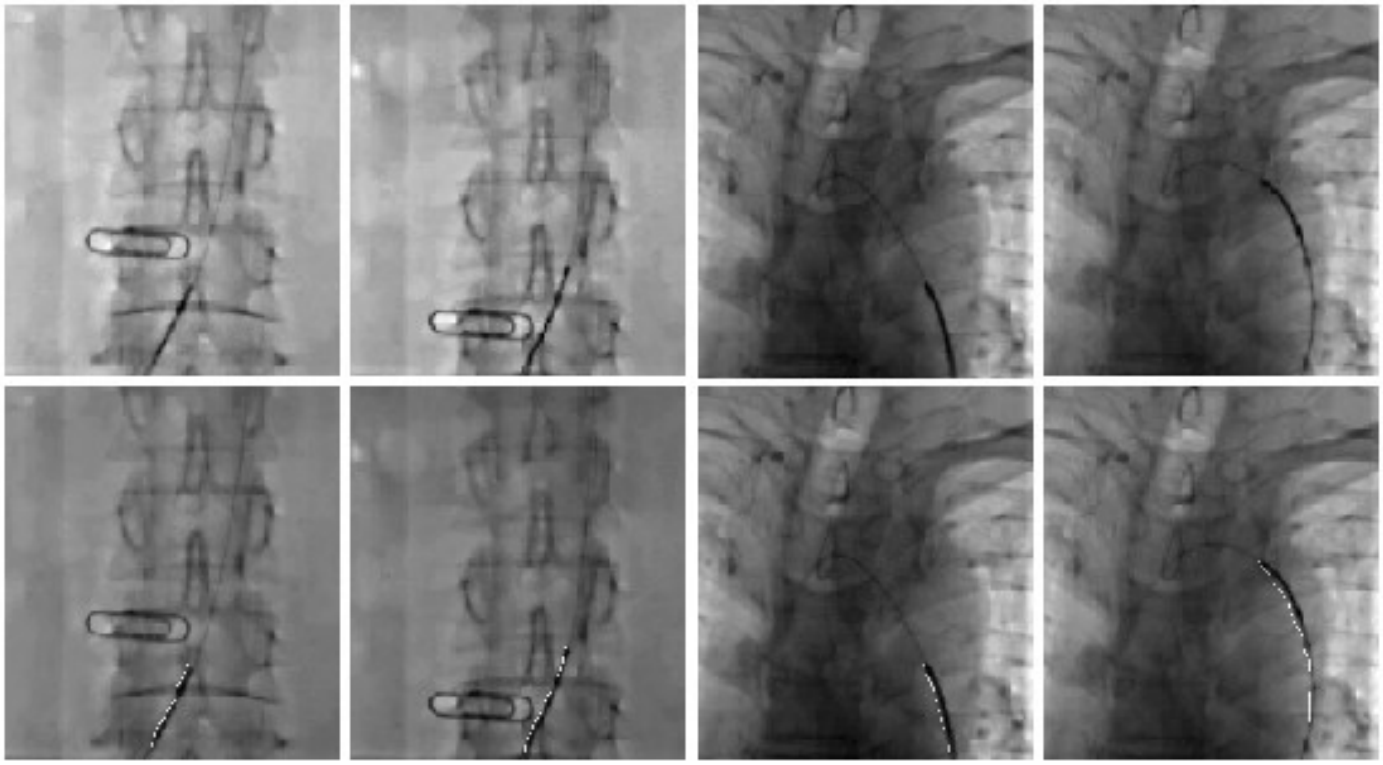

Fig. 7. True positive frames out of two sequences. The first and third rows are the origin images, the second and last rows are the output images.

As Fig. 7 depicts, the catheter is successfully detected and tracked. The lines in the figure are continuous, but the width is only one pixel, so they appear to be discontinuous. When the catheter overlaps with the bone suture, it is easy to introduce noise because of the similarities between structures and grayscale, so the curves in the images are not that smooth sometime. Yet spline fitting or machine learning methods can solve this problem, most of them can not meet the needs of surgical operations for real-time system.

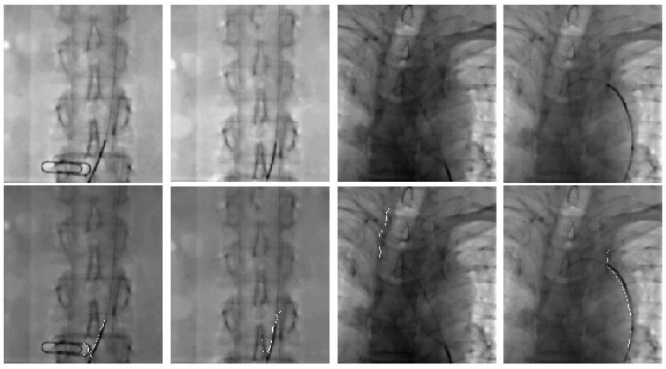

(a) (b) (c) (d)

Fig. 8. False positive frames out of two sequences. The first row is the origin images, the second row is the output images.

Fig.8 (c) shows the missed detection samples. In the post-processing of the image, we count the area of all connected domains in each frame, since in the most cases the catheter accounts for the largest area. In (c), the catheter only takes a small part, the texture of the vertebrae in the background image is significantly larger than that of catheter. So finally the catheter, detected while enhancing, is also ignored during post-processing. On account of the high temporal resolution (15.6 fps), missing one or two frames do not influence the surgeons. The other figures presents the false detection cases. The reason for the detection error is that the catheter is too close to the clip or bone edges, so the features are mixed in a low-resolution fluoroscope. At the same time, because we have applied closing to connect discontinuous parts, those adjacent edges may also be connected and can not be eliminated in post-processing.

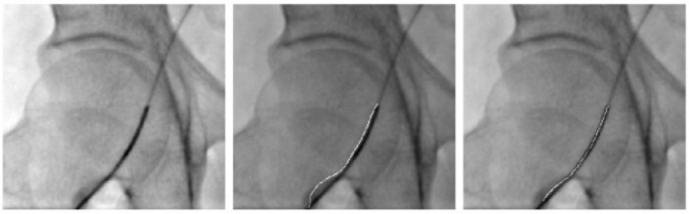

Fig. 9. The corrected catheter position

At the same time, it can be seen from the figure that the extracted position of the catheter is offset to the left from the actual position. This is because during the directional filtering, the sliding of the kernel function proceeds from left to right. In order to correct this deviation, we can filter it in an inverse method, as shown in the Fig. 9.

IV. CONCLUSIONS

In this paper, a catheter tracking method based on multi-scale filtering and direction-oriented algorithm is proposed.

The results indicate that the real-time catheter tracking based on the proposed method provides surgeons with better visual enhancement, which is beneficial to improve the surgical safety of current endovascular interventional surgery. The method detects the guide wire correctly in 89.36% of the frames and takes 0.064s per frame. By optimizing the code and using hardware solutions, a higher accuracy can be achieved without compromising the robustness and speed of the algorithm.

ACKNOWLEDGEMENTS

This research is partly supported by the National High Tech. Research and Development Program of China (No.2015AA04320, National Key Research and Development Program of China (2017YFB1304401).

REFERENCES

[1] Jian Guo, Xiaoliang Jin, Shuxiang Guo, "Study of the Operational Safety of a Vascular Interventional Surgical Robotic System", *Micromachines, Micromachines-262458*, doi: 10.3390/mi9030119, 2018.

[2] Xianqiang Bao, Shuxiang Guo, Nan Xiao, Youxiang Li, Cheng Yang, Yuhua Jiang, "A Cooperation of Catheters and Guidewires-based Novel Remote-Controlled Vascular Interventional Robot", *Biomedical Microdevices*, doi: 10.1007/s10544-018-0261-0, 2018.

[3] Zhang L, Guo S, Yu H, et al, "Design and performance evaluation of collision protection-based safety operation for a haptic robot-assisted catheter operating system", *Biomedical Microdevices*, Vol. 23, No.2, pp. 22, 2018.

[4] Yuan Wang, Shuxiang Guo, Nan Xiao, Youxiang Li and Yuhua Jiang, "Online Measuring and Evaluation of Guidewire Inserting Resistance for Robotic Interventional Surgery Systems", *Microsystem Technologies*, doi:10.1007/s00542-018-3750-4, 2018.

[5] Song Y, Guo S, Yin X, et al, "Design and performance evaluation of a haptic interface based on MR fluids for endovascular tele-surgery", *Microsystem Technologies*, No.2, pp. 1-10, 2018.

[6] Guo J, Guo S, Yu Y, "Design and characteristics evaluation of a novel teleoperated robotic catheterization system with force feedback for vascular interventional surgery", *Biomedical Microdevices*, Vol. 18, No.5, pp. 76, 2016.

[7] Yan Zhao, Shuxiang Guo, Nan Xiao, Yuxin Wang, Youxiang Li, Yuhua Jiang, "Operating Force Information On-line Acquisition of a Novel Slave Manipulator for Vascular Interventional Surgery", *Biomedical Microdevices*, doi: 10.1007/s10544-018-0275-7, 2018.

[8] Wang Y, Guo S, Tamiya T, et al, "A virtual-reality simulator and force sensation combined catheter operation training system and its preliminary evaluation", *Int J Med Robot*, Vol. 13, No.3, 2017.

[9] Zhang L, Guo S, Yu H, et al, "Performance evaluation of a strain-gauge force sensor for a haptic robot-assisted catheter operating system", *Microsystem Technologies*, Vol. 23, No.10, pp. 1-10, 2017.

[10] Fu Q, Guo S, Huang Q, et al, "Development and Evaluation of Novel Magnetic Actuated Microrobot with Spiral Motion Using Electromagnetic Actuation System", *Journal of Medical & Biological Engineering*, Vol. 36, No.4, pp. 1-9, 2016.

[11] Merrifield R, Taylor R, "The Surgical Robot Challenge [From the Guest Editors", *IEEE Robotics & Automation Magazine*, Vol. 24, No.2, pp. 22-23, 2017.

[12] Martel S, "Magnetic Navigation Control of Microagents in the Vascular Network: Challenges and Strategies for Endovascular Magnetic Navigation Control of Microscale Drug Delivery Carriers", *Control Systems IEEE*, Vol. 33, No.6, pp. 119-134, 20

[13] Szili-Torok T, Schwagten B, Akca F, "Catheter ablation of ventricular tachycardias using remote magnetic navigation: a consecutive case-control study", *Journal of Cardiovascular Electrophysiology*, Vol. 23, No.9, pp. 948, 2012.

[14] Chang P L, Rolls A, Praetere H D, "Robust Catheter and Guidewire Tracking Using B-Spline Tube Model and Pixel-Wise Posteriors", *IEEE Robotics & Automation Letters*, Vol. 1, No.1, pp. 303-308, 2017.

[15] Baert S A, Viergever M A, Niessen W J, "Guide-wire tracking during endovascular interventions", IEEE Trans Med Imaging, Vol. 22, No.8, pp. 965-972, 2003.

[16] Heibel H, Glocker B, Groher M, et al, "Interventional Tool Tracking Using Discrete Optimization", *IEEE Transactions on Medical Imaging*, Vol. 32, No.3, pp. 544-555, 2013.

[17] Wang C, Wang W, "A method for guide wire tracking in X-Ray angiographic images based on open active contours", *International Conference on Signal Processing. IEEE*, pp. 624-627, 2017.

[18] Fazlali H R, Karimi N, Soroushmehr S M, et al, "Robust catheter identification and tracking in X-ray angiographic sequences", *IEEE Engineering in Medicine and Biology Society. Annual Conference*, pp. 7901-7904, Aug, 2015.

[19] Slabaugh G, Kong K, Unal G, et al, "Variational Guidewire Tracking Using Phase Congruency", *International Conference on Medical Image Computing and Computer-Assisted Intervention*, Springer-Verlag, pp.612-619,2007.

[20] Zhang J, Dashtbozorg B, Bekkers E, et al, "Robust Retinal Vessel Segmentation via Locally Adaptive Derivative Frames in Orientation Scores", *IEEE Transactions on Medical Imaging*, Vol. 35, No.12, pp. 2631, 2016.

[21] Mohammed Shafeeq Ahmed, Baddam Indira, et al, "Morphological Technique for Detection of Microaneurysms from RGB Fundus Images", *IEEE WiSPNET 2017 conference*, pp. 44-47, 2017.

[22] Yang J, Ma S, Sun Q, et al, "Improved Hessian multiscale enhancement filter", *Bio-medical materials and engineering*, Vol. 24, No.6, pp. 3267-3275, 2014.

[23] Jian Zheng, Pei-Rong Lu et al, "Retinal Image Graph-Cut Segmentation Algorithm Using Multiscale Hessian-Enhancement-Based Nonlocal Mean Filter", *Computational and Mathematical Methods in Medicine*, Vol. 1, Aug, 2013.

[24] Xu X, Liu B, Zhou F, "Hessian-based vessel enhancement combined with directional filter banks and vessel similarity", 2013.

[25] Wang L, Xie X L, Bian G B, et al, "Guide-wire detection using region proposal network for X-ray image-guided navigation", *International Joint Conference on Neural Networks*, pp. 3169-3175, 2017.

[26] Barbu A, Athitsos V, Georgescu B, et al, "Hierarchical Learning of Curves Application to Guidewire Localization in Fluoroscopy", *Computer Vision and Pattern Recognition*, *2007. CVPR '07. IEEE Conference on. IEEE*, pp. 1-8, 2008.

[27] Hu J, Zheng B, Gao X, "Numerical evaluation of high-order singular boundary integrals using third-degree B-spline basis functions", *Wit Transactions on Modelling & Simulation*, 2014.

[28] Frangi A F, Niessen W J, Vincken K L, et al, "Multiscale vessel enhancement filtering", *Medical Image Computing and Computer-Assisted Interventation—MICCAI'98*, Springer Berlin , 1998.

[29] Saa S, Tang T B, Faye I, et al, "Blood vessel segmentation in color fundus images based on regional and Hessian features", *Graefes Archive for Clinical & Experimental Ophthalmology*, Vol. 255, No. 8, pp.1-9, 2017.

[30] Jin Jiaoying, "Segmentation of vascular tree in the medical images based on multiscale Hessian enhancement and active contour method", *Doctoral Dissertation*, 2014.

[31] Annunziata R, Garzelli A, Ballerini L, "Leveraging Multiscale Hessian-based Enhancement with a Novel Exudate Inpainting Technique for Retinal Vessel Segmentation", *IEEE Journal of Biomedical & Health Informatics*, Vol. 20, No. 4, pp.1129-1138, 2016.

[32] Shahzad A, Goh C M, Saad N M, et al, "Subcutaneous veins detection and backprojection method using Frangi vesselness filter", *Computer Applications & Industrial Electronics. IEEE*, pp. 65-68, 2015.

[33] Zheng Y J, Zhang Y H, Wang Z W, "Edge Detection Algorithm Based on the Eight Directions Sobel Operator", *Computer Science*, 2013.

[34] Furnari A, Farinella G M, Bruna A R, "Generalized Sobel Filters for gradient estimation of distorted images", *IEEE International Conference on Image Processing. IEEE*, pp. 3250-3254, 2015.

[35] Hui M, Oluwatoyin P P, Shuli S, "A finger vein recognition method using improved oriented filter and elastic registration", *Research Journal of Applied Sciences Engineering & Technology*, Vol. 6, No. 7, pp. 1153-1159, 2013.